Isotope effects and Born-Oppenheimer breakdown in excited singlet states of the lithium dimer

A. Adohi-Krou,[a] F. Martin, and A. J. Ross
Laboratoire de Spectrométrie Ionique et Moléculaire, CNRS et Université Lyon I (UMR 5579) Domaine Scientifique de la Doua, 69626 Villeurbanne, France

C. Linton
Department of Physics, University of New Brunswick, P.O. Box 4400, Fredericton, New Brunswick E3B 5A3, Canada

R. J. Le Roy
Guelph-Waterloo Centre for Graduate Work in Chemistry and Biochemistry, University of Waterloo, Waterloo, Ontario N2L 3G1, Canada

Observation of infrared electronic transitions involving the $1\,^1\Delta_g$ state of $^7\text{Li}_2$ has instigated an investigation of Born-Oppenheimer breakdown in four singlet electronic states correlating with $(2s+2s)$, $(2s+2p)$, and $(2p+2p)$ lithium atoms. The $1\,^1\Delta_g$ state, which correlates at long range with $(2p+2p)$ atoms, has been observed in emission from the $(5p)\,^1\Pi_u$ Rydberg state and in $1\,^1\Delta_g\text{-}B\,^1\Pi_u$ bands, in both instances following optical-optical double-resonance excitation. The latter transition was observed previously for the lighter isotopomer, $^6\text{Li}_2$ [C. Linton, F. Martin, P. Crozet, A. J. Ross, and R. Bacis, J. Mol. Spectrosc. **158**, 445 (1993)]. By analyzing multiple-isotopomer data for several electronic systems simultaneously, we have determined the electronic isotope shifts and the leading vibrational and/or rotational Born-Oppenheimer breakdown terms for the $X\,^1\Sigma_g^+$, $A\,^1\Sigma_u^+$, $B\,^1\Pi_u$, and $1\,^1\Delta_g$ states of the lithium dimer. This paper also reports Fourier transform measurements of the B-X absorption spectra of $^6\text{Li}_2$ and $^7\text{Li}_2$, which were required to better define the bottom portion of the $B\,^1\Pi_u$ state potential. © *2004 American Institute of Physics.* [DOI: 10.1063/1.1786920]

I. INTRODUCTION

A recent combined-isotopomer analysis of data for the A-X system of Li_2 has shown that Born-Oppenheimer breakdown (BOB) effects are significant in this nonhydride molecule.[1] They are dominated by an additive energy displacement between the $A\,^1\Sigma_u^+$ state potential curves for the different isotopomers, which correlates with the 0.33 cm^{-1} difference between the ^2P-^2S atomic transition energies in ^6Li and ^7Li (the value for ^7Li being larger).[2] The $B\,^1\Pi_u$-$X\,^1\Sigma_g^+$ system, whose upper state (as does the $A\,^1\Sigma_u^+$ state) correlates with $\text{Li}(2s\,^2\text{S})+\text{Li}(2p\,^2\text{P})$ atoms, is affected similarly, and isotope effects for this system have already been examined both through "conventional" parameter fits and through direct fits to determine the $B\,^1\Pi_u$ state potential energy and Born-Oppenheimer breakdown functions.[3] The objective of the present work is to report experimental data for the $1\,^1\Delta_g$ state, which correlates at long range with $\text{Li}(2p\,^2\text{P}_{3/2})+\text{Li}(2p\,^2\text{P}_{3/2})$ atoms, and to determine the pattern of Born-Oppenheimer breakdown effects among some excited singlet electronic states of the lithium dimer.

The $1\,^1\Delta_g$ state was observed previously in a study of the $1\,^1\Delta_g$-$B\,^1\Pi_u$ system of $^6\text{Li}_2$.[4] We have now used a slightly more elaborate experiment to access the $1\,^1\Delta_g$ state of the dominant isotopomer, $^7\text{Li}_2$, so a combined-isotopomer

analysis able to determine Born-Oppenheimer breakdown effects in this state[5] is now possible. However, because the $1\,^1\Delta_g$ state was observed only via transitions between excited electronic states (notably $1\,^1\Delta_g \rightarrow B\,^1\Pi_u$), secure descriptions of the $B\,^1\Pi_u$ and $X\,^1\Sigma_g^+$ states were essential for this study. Moreover, since the most detailed information about the $X\,^1\Sigma_g^+$ state comes from the extensively studied $A\,^1\Sigma_u^+$-$X\,^1\Sigma_g^+$ band system,[1] it was also necessary to include multiple-isotopomer A-X data in the present analysis. As a result, the analysis reported herein involves a simultaneous combined-isotopomer fit to data associated with transitions among five different electronic states.

II. EXPERIMENTAL DETAILS

Lithium molecules were produced in a heatpipe oven operating between 750 and 850 °C, using argon as a buffer gas (pressure typically 3–5 Torr). Since no B-X data for $^6\text{Li}_2$ were available in the literature, and the recent explorations of the $B\,^1\Pi_u$ state in $^7\text{Li}_2$ and $^6\text{Li}\,^7\text{Li}$ did not probe its lowest vibrational levels,[6,7] we have recorded these systems in absorption in the region 19 800–21 700 cm^{-1} using a Fourier transform spectrometer. This experiment effectively repeats the pioneering photographic work of Hessel and Vidal on the dominant isotopomer $^7\text{Li}_2$.[8] However, it was necessary to make new measurements if we were to avoid having to rely

---

[a] Permanent address: UFR SSMT Université de Cocody, (Abidjan) 22 Boîte Postale 582, Abidjan 22, Ivory Coast.
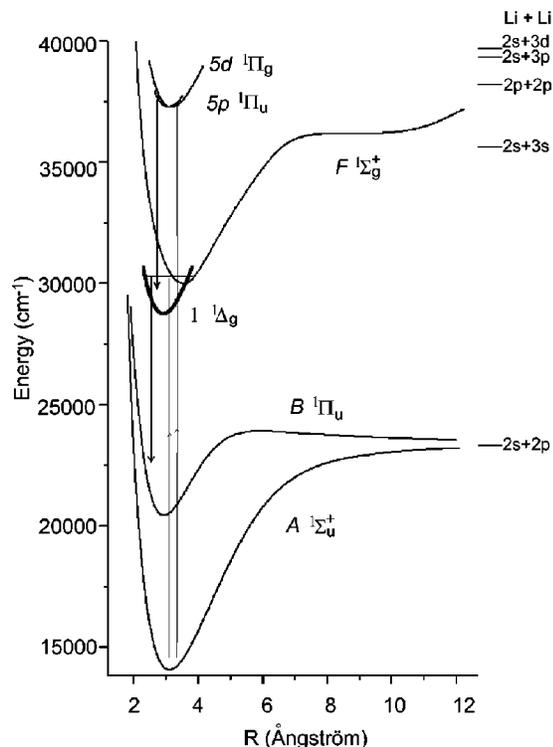
FIG. 1. Potential energy curves of states involved in the second step of optical-optical double resonance, collisional energy transfer and IR fluorescence. The $(5d)$ $^1\Pi_g$ and F $^1\Sigma_g^+$ states are populated by the laser (thin upwards arrows). The thicker downwards arrows indicate fluorescence seen following collisional energy transfer [from $(5d)$ $^1\Pi_g$ to the $(5p)$ $^1\Pi_u$ state, or from F $^1\Sigma_g^+$ to the 1 $^1\Delta_g$ state]. The curve for the F $^1\Sigma_g^+$ state is taken from an analysis by Pashov *et al.* (Ref. 17) based on measurements by Antonova *et al.* (Ref. 18) and that for the $(5d)$ $^1\Pi_g$ state is calculated from constants given by Bernheim (Ref. 19).

on synthetic $^7Li_2$ data generated from the Hessel-Vidal parameters,[8] as was done in earlier work,[6,3] since their original data set is not available.

In these absorption experiments, appropriate interference filters were used to select the desired input wavelengths from a 100 W halogen lamp source, and the interferograms were collected on a silicon avalanche detector. The response of the interferometer was first calibrated against the Doppler-limited I_2 absorption spectrum around 500 nm, in order to guard against possible systematic error. The metal samples were either 93% ^7Li (natural isotopic abundance), or an enriched sample of >95% ^6Li purchased from Eurisotope (Saclay, France). The absorption spectra are Doppler limited, and with the heatpipe running at 750 °C, measured linewidths were of the order of 0.15 cm^{-1}.

The 1 $^1\Delta_g$ state of $^7Li_2$ has been studied through collisionally induced fluorescence following two-color, single-mode double-resonance excitation. These experiments used higher heatpipe temperatures (typically 800–850 °C) and pressures to enhance the fluorescence signal. Two distinct excitation mechanisms were involved. In both cases, low lying vibrational levels of the A $^1\Sigma_u^+$ state were excited with emission from LD 700 dye around 680 nm (output power ~300 mW). One set of experiments then used DCM dye, operating around 660 nm to populate low vibrational levels of the F $^1\Sigma_g^+$ state (see Fig. 1). Excitation of $v'(F) = 0, 1,$
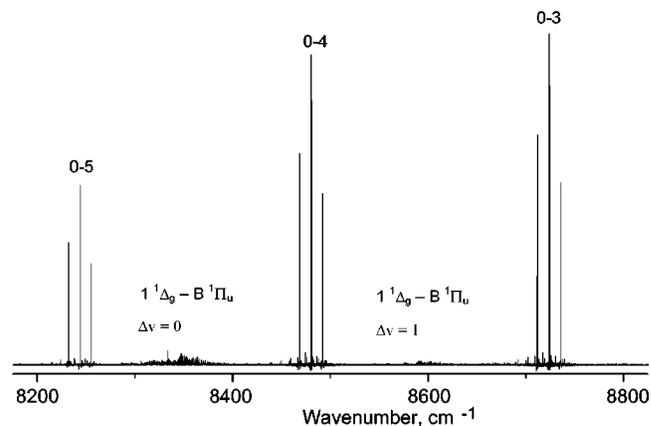

FIG. 2. Part of the infrared fluorescence recorded in $^7Li_2$ following double-resonance excitation of F $^1\Sigma_g^+ v = 0$, $J = 11$. Direct fluorescence gives $P(12)$, $Q(11)$, $R(10)$ triplets to the B $^1\Pi_u$ state, with some rotational relaxation. The weak bands around 8350 and 8600 cm^{-1} correspond to collisionally induced 1 $^1\Delta_g$-B $^1\Pi_u$ transitions.

and 2 gave strong direct fluorescence to the B $^1\Pi_u$ state between 1 and 1.4 μm, and in the same wavelength region, also to collisionally induced transitions assigned to the 1 $^1\Delta_g$ $\rightarrow B$ $^1\Pi_u$ system.

The second set of experiments used violet photons around 432 nm (typically 80 mW, from Stilbene 420 dye) to populate $v = 0$ or $v = 1$ levels of the $(5d)$ $^1\Pi_g$ Rydberg state by excitation from low vibrational levels of the A $^1\Sigma_u^+$ state. Direct fluorescence from this process consisted of $\Delta v = 0$, ± 1 progressions into both the C $^1\Pi_u$ state and the inner well of the 2 $^1\Sigma_u^+$ double-minimum state.[9] Collisional energy transfer from $v = 0$ of the $(5d)$ $^1\Pi_g$ Rydberg state populates a neighboring Rydberg state, believed to be $(5p)$ $^1\Pi_u$, and emission from it into $v = 0$ and 1 of the 1 $^1\Delta_g$ state is observed.[10] (Note that the Rydberg-state vibrational assignments are based only on rotational constants and approximate Franck-Condon factor calculations, and may not be definitive.) The electronic transitions involved are indicated in Fig. 1, and an example of collisionally induced fluorescence from the 1 $^1\Delta_g$ state into low vibrational levels of the B $^1\Pi_u$ state is shown in Fig. 2. The infrared fluorescence (6400–10 000 cm^{-1}) associated with these experiments was recorded on the Fourier transform spectrometer at an instrumental resolution of 0.08 cm^{-1} using an InGaAs detector, and a high pass optical filter served to remove A-X emission. The estimated uncertainty in the measured line positions is ten times smaller than the experimental resolution.

III. EXPERIMENTAL RESULTS

The treatment of our $B \leftarrow X$ absorption spectra was very straightforward, since both electronic states are known, and are essentially unperturbed. Only low vibrational levels were accessed in both states ($v'' \leq 3$ and $v' \leq 8$). These Doppler limited spectra were not fully resolved, and many overlapping lines were discarded from the data set.

The next step in the analysis was the study of the 1 $^1\Delta_g$ state of $^7Li_2$. Most of the relevant data are emission lines from levels $v = 0$–7 of the 1 $^1\Delta_g$ state, which were populated by collisional energy transfer from levels $v = 0, 1,$ and 2

of the $F\,^1\Sigma_g^+$ state. The excitation process was highly selective, since it involves pumping molecules into a chosen v, J level in $F\,^1\Sigma_g^+$, but the collisional energy transfer process is less restrictive and many rotational lines are observed (see Fig. 2). The latter step retains only the overall symmetry label (a or s) resulting from nuclear spin, electronic, and rotational symmetry properties, and allows several rotational lines to be observed in one Fourier transform (FT) record. Energy transfer is most efficient when the vibrational levels of the $F\,^1\Sigma_g^+$ state and the $1\,^1\Delta_g$ state are close in energy. This explains why the (4-4) band depicted in Fig. 2 is stronger than the others. The transitions involving upper state levels in which J changes only by 0 or ±1 in the collisional transfer are somewhat stronger than the others. This can be seen from the enhancement of $R(11)$, $Q(12)$, and $P(13)$ lines in Fig. 2. The strongest transitions are those with $\Delta v = 0$, but some weaker $\Delta v = \pm1$ bands were also observed. Overall, some 1596 lines were recorded in the $1\,^1\Delta_g \rightarrow B\,^1\Pi_u$ system of $^7\text{Li}_2$, involving rotational levels with $2 \leqslant J \leqslant 51$.

Although Figs. 2 and 3 show that this system is quite congested, making line assignments in the less overlapped regions was reasonably straightforward, based on known parity selection rules and published rotational constants for the $1\,^1\Delta_g$ state of $^6\text{Li}_2$.[4] Nuclear spin symmetry is conserved in the energy transfer between electronic states. Because the OODR excitation scheme was selective in populating only one level of the $F\,^1\Sigma_g^+$ state at a time, the starting point was either the subset of s symmetry levels in $1\,^1\Delta_g$ if the double resonance populated an even-J level in the $F\,^1\Sigma_g^+$ state, or the a symmetry levels if an odd-J F-state level were populated. Nuclear spin statistics produce stronger spectra for the s species (the s:a ratio is 10:6 for $^7\text{Li}_2$). After excitation of an even-J level in the $F\,^1\Sigma_g^+$ state, we observe the following.

(i) Only s levels of the $1\,^1\Delta_g$ state are populated by collision, so only s levels are involved in $1\,^1\Delta_g \rightarrow B\,^1\Pi_u$ fluorescence.
(ii) There are no restrictions on J in the $1\,^1\Delta_g \rightarrow B\,^1\Pi_u$ system, but transitions to levels with *odd J''* (R, P, and Q lines) involve e parity levels of $B\,^1\Pi_u$, while *even J''* transitions involve f parity levels of $B\,^1\Pi_u$.

Populating a levels of the $F\,^1\Sigma_g^+$ state allows the opposite parity components to be observed. A smaller amount of information came from transitions into $v = 0-2$ of the $1\,^1\Delta_g$ state (250 lines, $3 \leqslant J \leqslant 32$) from levels $v = 0$ and 1 of the $(5p)\,^1\Pi_u$ state located $\sim37\,260$ cm^{-1} above the electronic ground state. Once again, conservation of nuclear spin symmetry allows access to either s or a levels in the Rydberg $^1\Pi_u$ state through collisions, according to whether the initial level in the $X\,^1\Sigma_g^+$ ground state was s (even J) or a (odd J), but in the subsequent $(5p)\,^1\Pi_u \rightarrow 1\,^1\Delta_g$ transition, both odd- and even-J'' levels are observed. The nine observed vibrational levels of the $1\,^1\Delta_g$ state appear to be unperturbed, and there is no discernable Λ doubling (Fig. 3).

In addition to our information on the $1\,^1\Delta_g$ state, resolved fluorescence from the F-state levels pumped in the initial excitation process yielded data on both the $A\,^1\Sigma_u^+$ and $B\,^1\Pi_u$ states. Similarly, fluorescence from the initially ex-
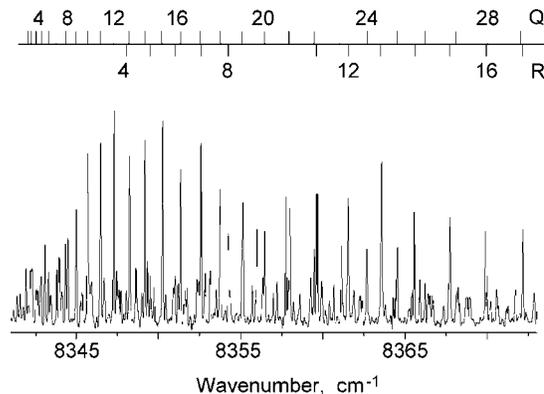

FIG. 3. Closeup view of the $1\,^1\Delta_g$-$B\,^1\Pi_u$ transition near 8350 cm^{-1}. The strongest lines are the R and Q lines of the (4-4) band. The weaker ones come from other bands in the $\Delta v = 0$ sequence.

cited $A\,^1\Sigma_u^+$ state levels yielded additional information on the first dozen vibrational levels of the $X\,^1\Sigma_g^+$ state of the two homonuclear isotopomers. These results are summarized, together with all of the other data used in our analysis, in Table I.

IV. ANALYSIS: COMBINED-ISOTOPOMER FITS

In our study of isotope effects in excited states of the lithium dimer, all molecular energies are quoted with respect to an energy zero at $v = -1/2$ in the $X\,^1\Sigma_g^+$ state of the dominant isotopomer $^7\text{Li}_2$. Although our combination of absorption spectroscopy and resolved laser induced fluorescence covers a wide selection of vibrational levels, parts of both the A-X and B-X systems have been investigated by higher resolution techniques by other groups. Wherever possible, we have also included raw wavenumber measurements from other sources to complement our own measurements. The origins of the data for the three isotopomers of the lithium dimer are also indicated in Table I. Note that there are no observations of the $1\,^1\Delta_g$ state in $^6\text{Li}\,^7\text{Li}$, although the OODR experiment did furnish limited observations of the $F\,^1\Sigma_g^+ \rightarrow B\,^1\Pi_u$ system for this species. Some $F\,^1\Sigma_g^+ \rightarrow A\,^1\Sigma_u^+$ transitions to low A-state vibrational levels of $^6\text{Li}_2$ and $^7\text{Li}_2$ were also included in this fit (none have been recorded to low vibrational levels of the A-state $^6\text{Li}\,^7\text{Li}$ molecule). The complete list of lines used in this work has been supplied to this Journal's electronic data archive.[11]

The analysis used the program DPARFIT (Ref. 12) to perform a simultaneous combined-isotopomer fit to all of the data for the several electronic systems listed in Table I. The input file contained 14 621 measured lines, and involved three isotopomers and five electronic states. Each experimental datum was weighted by the inverse square of the estimated uncertainty indicated in Table I.

Energy levels of the $X\,^1\Sigma_g^+$, $A\,^1\Sigma_u^+$, $B\,^1\Pi_u$, $1\,^1\Delta_g$, and $(5p)\,^1\Pi_u$ states for a particular isotopomer α were represented by $Y_{\ell,m}$ Dunham coefficients:

$$E^{(\alpha)}(v,J) = \sum_{m=0}^{m_{\max}} \sum_{l=0}^{l_{\max}} Y_{l,m}^{(\alpha)}(v+1/2)^l [J(J+1) - \Omega^2]^m.$$

(1)

TABLE I. Résumé of the Li$_2$ data used in the present unified multiple-isotopomer multiple-state analysis.

System	Lines	Uncertainty (cm^{-1})	Type of experiment	v' range	v'' range	J'' range
			^{6}Li$_2$			
$A\,^1\Sigma_u^+ - X\,^1\Sigma_g^+$	2014	0.01	FT absorption[a]	0–13	0–2	0–71
$A\,^1\Sigma_u^+ - X\,^1\Sigma_g^+$	932	0.005	Polarization spectroscopy[b]	0–24	0–7	0–43
$A\,^1\Sigma_u^+ - X\,^1\Sigma_g^+$	1403	0.006	FT resolved fluorescence	···	0–13	1–52
$B\,^1\Pi_u - X\,^1\Sigma_g^+$	1241	0.02	FT absorption	0–5	0–2	0–60
$I\,^1\Delta_g - B\,^1\Pi_u$	831	0.008	OODR+collisions (FTS)	0–5	0–6	1–58
$F\,^1\Sigma_g^+ - B\,^1\Pi_u$	387	0.005	FT resolved fluorescence	···	0–15	1–42
$F\,^1\Sigma_g^+ - A\,^1\Sigma_u^+$	82	0.008	FT resolved fluorescence	···	1–13	3–14
			^{7}Li$_2$			
$A\,^1\Sigma_u^+ - X\,^1\Sigma_g^+$	1365	0.01	FT absorption[a]	0–13	0–3	0–64
$A\,^1\Sigma_u^+ - X\,^1\Sigma_g^+$	1415	0.02	Absorption[c]	0–6	0–13	1–44
$A\,^1\Sigma_u^+ - X\,^1\Sigma_g^+$	1084	0.006	FT resolved fluorescence	···	0–12	2–41
$B\,^1\Pi_u - X\,^1\Sigma_g^+$	1129	0.015	FT absorption	0–8	0–3	0–66
$B\,^1\Pi_u - X\,^1\Sigma_g^+$	167	0.002	Sub-Doppler absorption[d]	3–8	0–3	0–62
$1\,^1\Delta_g - B\,^1\Pi_u$	1596	0.008	OODR+collisions (FTS)	0–7	0–6	2–51
$F\,^1\Sigma_g^+ - B\,^1\Pi_u$	176	0.008	FT resolved fluorescence	···	0–8	2–26
$F\,^1\Sigma_g^+ - A\,^1\Sigma_u^+$	149	0.008	FT resolved fluorescence	···	0–24	18–23
$(5p)\,^1\Pi_u - 1\,^1\Delta_g$	250	0.008	OODR+collisions (FTS)[e]	0–1	0–1	3–32
			^{6}Li$\,^7$Li			
$A\,^1\Sigma_u^+ - X\,^1\Sigma_g^+$	224	0.005	Polarization spectroscopy[b]	0–5	0–3	0–40
$B\,^1\Pi_u - X\,^1\Sigma_g^+$	29	0.002	Sub-Doppler absorption[f]	6–8	0–2	4–60
$F\,^1\Sigma_g^+ - B\,^1\Pi_u$	128	0.005	FT resolved fluorescence	···	0–8	11–32

[a]Reference 1.
[b]Reference 20.
[c]Reference 21.
[d]Reference 6.
[e]Reference 10.
[f]Reference 7.

For the $B\,^1\Pi_u$ and Rydberg $(5p)\,^1\Pi_u$ states, an additional term is added to Eq. (1) to take account of Λ doubling:

$$\mathrm{sg}(e/f)\sum_{l=0}\sum_{m=1} q_{l,m}^{(\alpha)}(v+1/2)^l[J(J+1)]^m. \qquad (2)$$

For the $B\,^1\Pi_u$ state the Λ doubling is mainly due to interactions with the nearby $A\,^1\Sigma_u^+$ state, so the coefficient $\mathrm{sg}(e/f)$ is $+1$ for e parity levels, and 0 for the f parity levels (which are therefore unaffected by the Λ-doubling perturbation). On the other hand, since the origin of the perturbation is unknown for the Rydberg $^1\Pi_u$ state, Λ-doubling perturbations for this Rydberg state were defined with respect to the e/f $\mathrm{sg}(e)=+1/2$ for e parity levels and $\mathrm{sg}(f)=-1/2$ for f parity levels for this state.

The isotopic dependence of the $Y_{l,m}$ Dunham coefficients for isotopomer α of a diatomic molecule AB formed from atoms of mass $M_A^{(\alpha)}$ and $M_B^{(\alpha)}$ is given by

$$Y_{l,m}^{(\alpha)}=\left\{ Y_{l,m}^{(1)}+\frac{\Delta M_A^{(\alpha)}}{M_A^{(\alpha)}}\delta_{l,m}^A+\frac{\Delta M_B^{(\alpha)}}{M_B^{(\alpha)}}\delta_{l,m}^B\right\}\left(\frac{\mu_1}{\mu_\alpha}\right)^{m+l/2}, \qquad (3)$$

where $Y_{l,m}^{(1)}$ is the value for the "reference" isotopomer (chosen here to be ^{7}Li$_2$), and $\Delta M_{A,B}^{(\alpha)}=M_{A,B}^{(\alpha)}-M_{A,B}^{(1)}$.[5] In the present case both atoms are lithium, so only one set of BOB coefficients arises, which means that $\delta_{l,m}^A=\delta_{l,m}^B=\delta_{l,m}^{Li}$. Similarly, the isotopomer dependence of the Λ-doubling expansion coefficients is given by the simple first-order semiclassical mass-scaling relationship

$$q_{l,m}^{(\alpha)}=q_{l,m}^{(1)}\left(\frac{\mu_1}{\mu_\alpha}\right)^{m+l/2}, \qquad (4)$$

where μ_α is the usual reduced mass of isotopomer α of molecule A-B.

An empirically determined additive shift of all levels of isotopomer α in electronic state S is given by

$$\Delta T_{v=-1/2}^{(\alpha)}(S)=\left\{\frac{\Delta M_A^{(\alpha)}}{M_A^{(\alpha)}}+\frac{\Delta M_B^{(\alpha)}}{M_B^{(\alpha)}}\right\}\delta_{0,0}^{Li}(S). \qquad (5)$$

However, unless the isotope dependence of the well depth (D_e) is experimentally determined for at least one of the electronic states, empirical fits can only determine the *differences* between these additive isotope shifts for the various electronic states. In the present work all such differences are expressed with the $X\,^1\Sigma_g^+$ state as a reference. Thus, for electronic state S the fit yields an *effective* isotope shift coefficient defined as

$$\widetilde{\delta}_{0,0}^{Li}(S)\equiv\delta_{0,0}^{Li}(S)-\delta_{0,0}^{Li}(X). \qquad (6)$$

The associated electronic isotope shift would then be written as $\Delta\widetilde{T}_{v=-1/2}^{(\alpha)}(S)\equiv\Delta T_{v=-1/2}^{(\alpha)}(S)-\Delta T_{v=-1/2}^{(\alpha)}(X)$. Our results show that these constant (i.e., independent of v and J) terms dominate the Born-Oppenheimer breakdown effects in all of these states, although contributions from $\delta_{1,0}^{Li}$ and/or $\delta_{0,1}^{Li}$ were usually also significant.

The available data set offers a comprehensive picture of the $B\,^1\Pi_u$ state, but involves a smaller selection of vibrational levels in the $X\,^1\Sigma_g^+$, $A\,^1\Sigma_u^+$, and $1\,^1\Delta_g$ states. How-

TABLE II. Dunham parameters ($Y_{l,m}$) and Born-Oppenheimer breakdown parameters ($\delta_{l,m}$) for the electronic ground state $X\,^1\Sigma_g^+$ of the lithium dimer, valid up to $v=13$. The electronic isotope shift is assumed to be zero for this state. All parameters are quoted in cm^{-1}. Parameters for ^{7}Li$_2$ are quoted with two standard deviation uncertainties (given in parenthesis) in units of the last digit shown.

Parameter	Fitted value ^{7}Li$_2$	Calculated value ^{6}Li$_2$	Calculated value ^{6}Li ^{7}Li
$\tilde{T}_{v=-1/2}$	0.0	0.0	0.0
$Y_{1,0}$	351.404 90(170)	379.514 344 8	365.729 852 9
$Y_{2,0}$	$-2.582\,89(71)$	$-3.012\,668\,06$	$-2.797\,779\,03$
$10^3\,Y_{3,0}$	$-5.848(120)$	$-7.366\,741$	$-6.592\,78$
$10^3\,Y_{4,0}$	$-0.131(10)$	$-0.178\,222\,3$	$-0.153\,704\,4$
$10^3\,Y_{5,0}$	$-0.0061(3)$	$-0.008\,962\,79$	$-0.007\,449\,01$
$Y_{0,1}$	0.672 526 2(79)	0.784 430 697	0.728 478 448
$10^3\,Y_{1,1}$	$-7.0423(26)$	$-8.871\,204\,3$	$-7.939\,182\,3$
$10^3\,Y_{2,1}$	$-0.031\,53(61)$	$-0.042\,895\,79$	$-0.036\,994\,65$
$10^7\,Y_{3,1}$	$-6.8(6)$	$-9.991\,31$	$-8.303\,81$
$10^7\,Y_{4,1}$	$-0.566(21)$	$-0.898\,158$	$-0.719\,348$
$10^6\,Y_{0,2}$	$-9.7939(50)$	$-13.324\,362$	$-11.491\,339\,7$
$10^6\,Y_{1,2}$	$-0.0427(15)$	$-0.062\,739\,5$	$-0.052\,143\,1$
$10^{10}\,Y_{2,2}$	$-6.0(20)$	-9.5211	-7.6256
$10^{10}\,Y_{3,2}$	$-1.47(10)$	$-2.519\,28$	$-1.944\,44$
$10^{10}\,Y_{0,3}$	1.336(11)	2.120 033	1.697 966
$10^{13}\,Y_{1,3}$	18.3(23)	31.362	24.206
$10^{13}\,Y_{2,3}$	$-1.5(3)$	-2.7763	-2.065
$10^{13}\,Y_{0,4}$	$-0.0104(9)$	$-0.019\,249$	$-0.014\,317\,4$
$10^3\,\delta_{1,0}$	5.6(5)		

ever, because of this range and the unusual (barrier) shape of the B-state potential, fitting all available $B\,^1\Pi_u$ state data to Dunham expansions requires quite high-order polynomials for rotation, centrifugal distortion, Λ-doubling, and Born-Oppenheimer breakdown effects. This in turn causes the values of the leading low-order parameters which characterize the shape of the potential near its minimum to be unusually sensitive to the chosen polynomial orders, while high interparameter correlation leads to anomalously large parameter uncertainties. For example, the present analysis yields $Y_{10}=270.877(\pm0.004)$ cm^{-1}, while the comprehensive B-state analysis of Huang and Le Roy,[3] which found that representing all 18 vibrational levels required a 14th order polynomial, obtained $Y_{10}=271.8(\pm0.6)$ cm^{-1}. Because of our particular interest in defining both the shape of the potential well and BOB effects around the potential minimum, we chose to restrict the present fits to consider only data involving B-state levels with $v\leq8$, thus minimizing those problems. Similarly, the available $A\,^1\Sigma_u^+$ state data extend most of the way to dissociation,[13–15] and interparameter correlation again gives rise to large uncertainties in the low-order Dunham coefficients if all data are included. To facilitate an optimum determination of BOB behavior near the $A\,^1\Sigma_u^+$ state potential minimum, the range of $A\,^1\Sigma_u^+$ data used in the present analysis was therefore limited to $v(A)=0-24$.

The resulting simultaneous multiple-isotopomer fit to the five-state data set summarized in Table I yielded the parameter sets for the $X\,^1\Sigma_g^+$, $A\,^1\Sigma_u^+$, $B\,^1\Pi_u$, $1\,^1\Delta_g$, and $(5p)\,^1\Pi_u$ electronic states listed in Tables II–VI, respectively. As mentioned above, absolute energies are quoted with respect to an energy zero at $E(v=-1/2,J=0)$ in the $X\,^1\Sigma_g^+$ state of ^{7}Li$_2$. This fit to 14 621 data had an overall dimensionless root-mean-square deviation $\overline{dd}_{tot}=1.08$, and determined 357 parameters, of which 92 were Dunham-type expansion parameters and the remainder fluorescence series origins. On

request, program DPARFIT applies a sequential rounding and refitting procedure which minimizes the numbers of significant digits required for all of the free parameters determined by the fit (here, Dunham-type parameters for the reference isotopomer ^{7}Li$_2$ and fluorescence series origins for all isotopomers) with no loss of precision. However, the derived parameter values [see Eqs. (3) and (5)] for the "minor isotopomer" species ^{6}Li$_2$ and ^{6}Li ^{7}Li (see Tables II–VI) typically require more significant digits than the rounded values for the dominant isotopomer to provide a consistent level of precision in representing the input data.[5]

The overall contribution of the Born-Oppenheimer breakdown terms was assessed in fits in which some or all of these parameters were neglected. If all BOB parameters are omitted, the resulting fit yields a dimensionless root-mean-square deviation of $\overline{dd}_{tot}=7.03$ and systematic "calc-obs" deviations, the latter including average dimensionless deviations of -6.3 for the A-X system of ^{7}Li$_2$ and $+4.5$ for the A-X system of ^{6}Li$_2$. Allowing the $\tilde{\delta}_{0,0}$ electronic parameters to be fitted for the $A\,^1\Sigma_u^+$, $B\,^1\Pi_u$, and $1\,^1\Delta_g$ states substantially improved the fit, yielding $\overline{dd}_{tot}=1.30$, and reoptimizing the orders of all the various Dunham expansions fails to improve the $\overline{dd}_{tot}$ beyond 1.28. If the fit also varies $\delta_{1,0}$ parameters (i.e., includes both electronic and vibrational BOB terms) for those states for which statistically significant values can be determined, it yields $\overline{dd}_{tot}=1.23$. Similarly, a fit which allows only electronic and rotational Born-Oppenheimer breakdown terms $\tilde{\delta}_{0,0}$ and $\delta_{0,1}$ yields $\overline{dd}_{tot}=1.15$. Our final recommended fit, which included fitted electronic, vibrational, and rotational BOB terms, has $\overline{dd}_{tot}=1.08$.

While small values of the leading vibrational or rotational Born-Oppenheimer breakdown coefficients $\delta_{\ell,m}$ were determined for most of the electronic states considered, by

TABLE III. Dunham ($Y_{l,m}$) and Born-Oppenheimer breakdown parameters ($\delta_{l,m}$) for the $A\,^1\Sigma_u^+$ state of the lithium dimer, valid up to $v = 24$. All parameters are quoted in cm^{-1}. Parameters for $^7\text{Li}_2$ are quoted with two standard deviation uncertainties (given in parenthesis) in units of the last digit shown.

Parameter	Fitted value $^7\text{Li}_2$	Calculated value $^6\text{Li}_2$	Calculated value $^6\text{Li}\,^7\text{Li}$
$\widetilde{T}_{v=-1/2}$	14 068.2994(22)	14 068.1843	14 068.2418
$Y_{1,0}$	255.4771(25)	275.911 785 2	265.890 928 9
$Y_{2,0}$	$-1.580\,652(1100)$	$-1.843\,663\,41$	$-1.712\,157\,71$
$10^3\,Y_{3,0}$	1.75(22)	2.204 48	1.972 873 8
$10^3\,Y_{4,0}$	0.18(2)	0.244 885 6	0.211 196 88
$10^6\,Y_{5,0}$	$-14.8971(1300)$	$-21.888\,458$	$-18.191\,583$
$10^6\,Y_{6,0}$	0.4032(350)	0.639 8183	0.512 440 0
$10^9\,Y_{7,0}$	$-4.52(38)$	$-7.746\,352$	$-5.978\,809$
$Y_{0,1}$	0.497 449 4(76)	0.580 193 011	0.538 822 244
$10^3\,Y_{1,1}$	$-5.4830(16)$	$-6.906\,949\,9$	$-6.181\,295\,4$
$10^6\,Y_{2,1}$	23.527(360)	32.007 91	27.604 61
$10^6\,Y_{3,1}$	$-0.556(39)$	$-0.816\,936$	$-0.678\,959$
$10^9\,Y_{4,1}$	6.0(20)	9.521 11	7.6256
$10^9\,Y_{5,1}$	$-0.265(32)$	$-0.454\,156$	$-0.350\,528$
$10^6\,Y_{0,2}$	$-7.4961(41)$	$-10.198\,261$	$-8.795\,294$
$10^6\,Y_{1,2}$	0.0609(4)	0.089 481	0.074 368
$10^9\,Y_{2,2}$	$-0.66(4)$	$-1.047\,32$	$-0.838\,82$
$10^9\,Y_{3,2}$	$-0.022(2)$	$-0.037\,703$	-0.0291
$10^9\,Y_{0,3}$	0.1027(6)	0.162 969 6	0.130 524 8
$10^9\,Y_{1,3}$	$-0.001\,02(4)$	$-0.001\,748\,07$	$-0.001\,349\,2$
$\widetilde{\delta}_{0,0}$	0.346(4)		
$10^3\,\delta_{1,0}$	7.8(5)		
$10^5\,\delta_{0,1}$	7.5(2)		

TABLE IV. Dunham ($Y_{l,m}$), Λ-doubling ($q_{l,m}$), and Born-Oppenheimer breakdown ($\delta_{l,m}$) parameters for the $B\,^1\Pi_u$ state of the lithium dimer, valid up to $v = 8$. All parameters are quoted in cm^{-1}. Parameters for $^7\text{Li}_2$ are quoted with two standard deviation uncertainties (given in parenthesis) in units of the last digit shown.

Parameter	Fitted value $^7\text{Li}_2$	Calculated value $^6\text{Li}_2$	Calculated value $^6\text{Li}\,^7\text{Li}$
$\widetilde{T}_{v=-1/2}$	20 436.2446(40)	20436.0166	20 436.1306
$Y_{1,0}$	270.876 58(440)	292.545 986 1	281.919 559 1
$Y_{2,0}$	$-3.086\,55(170)$	$-3.600\,134\,19$	$-3.343\,342\,1$
$10^3\,Y_{3,0}$	$-17.1(3)$	$-21.540\,92$	$-19.277\,80$
$10^3\,Y_{4,0}$	$-2.0668(130)$	$-2.811\,831$	$-2.425\,01$
$Y_{0,1}$	0.557 439 6(210)	0.650 194 348	0.603 816 974
$10^3\,Y_{1,1}$	$-8.690(13)$	$-10.946\,816\,4$	$-9.796\,727\,5$
$10^6\,Y_{2,1}$	11.(5)	14.965 23	12.906 48
$10^6\,Y_{3,1}$	$-31.953(870)$	$-46.948\,862$	$-39.019\,382$
$10^6\,Y_{4,1}$	2.487(85)	3.946 498	3.160 809 2
$10^6\,Y_{5,1}$	$-0.115(3)$	$-0.197\,086\,4$	$-0.152\,115\,7$
$10^6\,Y_{0,2}$	$-9.4973(300)$	$-12.920\,845$	$-11.143\,334$
$10^6\,Y_{1,2}$	0.103(11)	0.151 338 9	0.125 778 4
$10^6\,Y_{2,2}$	$-0.066\,63(220)$	$-0.105\,731\,87$	$-0.084\,682\,24$
$10^9\,Y_{3,2}$	6.535(240)	11.199 649	8.644 141
$10^9\,Y_{4,2}$	$-0.361(10)$	$-0.668\,172\,6$	$-0.496\,978$
$10^9\,Y_{0,3}$	0.1534(190)	0.243 422 9	0.194 961 1
$10^9\,Y_{1,3}$	$-0.0743(45)$	$-0.127\,334\,95$	$-0.098\,279\,98$
$10^{13}\,Y_{2,3}$	126.99(450)	235.045	174.823 38
$10^{13}\,Y_{3,3}$	$-8.13(21)$	$-16.251\,55$	$-11.648\,62$
$10^{13}\,Y_{0,4}$	$-0.116(52)$	$-0.214\,704$	$-0.159\,694$
$10^{13}\,Y_{1,4}$	0.1074(91)	0.214 688 3	0.153 882 1
$10^{13}\,Y_{2,4}$	$-0.0108(5)$	$-0.023\,315\,82$	$-0.016\,105\,02$
$10^{18}\,Y_{0,5}$	0.7(5)	1.511 21	1.043 84
$10^{18}\,Y_{1,5}$	$-0.59(8)$	$-1.375\,63$	$-0.915\,679$
$10^6\,q_{0,1}$	201.3(10)	273.864	236.189
$10^6\,q_{1,1}$	$-3.9(1)$	-5.7303	-4.7625
$10^6\,q_{0,2}$	$-0.0153(4)$	$-0.028\,319$	$-0.021\,063$
$\widetilde{\delta}_{0,0}$	0.685(4)		

TABLE V. Dunham parameters ($Y_{l,m}$) and Born-Oppenheimer breakdown parameters ($\delta_{l,m}$) for the $1\,{}^1\Delta_g$ state of the lithium dimer, valid up to $v=9$. All parameters are quoted in cm^{-1}. Parameters for ${}^7Li_2$ are quoted with two standard deviation uncertainties (given in parenthesis) in units of the last digit shown.

Parameter	Fitted value ${}^7Li_2$	Calculated value ${}^6Li_2$	Calculated value ${}^6Li\,{}^7Li$
$\widetilde{T}_{v=-1/2}$	28 746.3101(37)	28 745.8645	28 746.0873
$Y_{1,0}$	271.4855(25)	293.203 618	282.553 303
$Y_{2,0}$	−1.714 38(69)	−1.999 643	−1.857 011 5
$10^3\,Y_{3,0}$	5.37(6)	6.7646	6.0539
$Y_{0,1}$	0.567 688 1(160)	0.662 176 86	0.614 931 457
$10^3\,Y_{1,1}$	−3.6766(33)	−4.631 423	−4.144 839
$10^3\,Y_{2,1}$	0.0287(2)	0.039 045 6	0.033 674 2
$10^6\,Y_{0,2}$	−9.8265(190)	−13.368 713	−11.529 59
$10^6\,Y_{1,2}$	−0.1958(34)	−0.287 691	−0.239 101
$10^{10}\,Y_{0,3}$	2.136(82)	3.389 51	2.714 71
$10^{10}\,Y_{1,3}$	0.191(11)	0.327 33	0.252 64
$10^{15}\,Y_{0,4}$	−4.2(11)	−7.7738	−5.7820
$\delta_{0,0}$	1.339(5)		
$10^5\,\delta_{0,1}$	−7.4(4)		

far the largest BOB effects are those associated with the coefficients $\widetilde{\delta}_{0,0}$. For isotopomer α, the total energy at the potential minimum of a given electronic state is

$$T_e^{(\alpha)} = T_{v=-1/2}^{(1)} + \Delta T_{v=-1/2}^{(\alpha)} - Y_{0,0}^{(\alpha)}, \qquad (7)$$

where $\Delta T_{v=-1/2}^{(\alpha)}$ is the empirically determined quantity given by Eq. (5) and $Y_{0,0}^{(\alpha)}$ is the correction to the first-order semiclassical quantization condition which takes account of the fact that the potential energy minimum usually does not precisely correspond to vibrational quantum number $v=-1/2$. Higher-order semiclassical theory[16] shows that $Y_{0,0}^{(\alpha)}$ may be accurately approximated by the expression

$$Y_{00} = \frac{Y_{01}+Y_{20}}{4} - \frac{Y_{11}Y_{10}}{12Y_{01}} + \left(\frac{1}{Y_{01}}\right)\left(\frac{Y_{11}Y_{10}}{12Y_{01}}\right)^2. \qquad (8)$$

For a general diatomic molecule, the total isotope shift of the potential energy minimum of a given electronic state is therefore

$$\Delta T_e^{(\alpha)} = \left(\frac{\Delta M_A^{(\alpha)}}{M_A^{(\alpha)}}\right)\delta_{0,0}^A + \left(\frac{\Delta M_B^{(\alpha)}}{M_B^{(\alpha)}}\right)\delta_{0,0}^B - \Delta Y_{0,0}^{(\alpha)}, \qquad (9)$$

where $\Delta T_e^{(\alpha)} = T_e^{(\alpha)} - T_e^{(1)}$ and $\Delta Y_{0,0}^{(\alpha)} = Y_{0,0}^{(\alpha)} - Y_{0,0}^{(1)}$. In the present case, the fact that the differences between the poten-

tial energy well depths for different isotopomers have not been determined accurately for any of these electronic states means that Eq. (9) must be replaced by

$$\Delta \widetilde{T}_e^{(\alpha)} = \left[\left(\frac{\Delta M_A^{(\alpha)}}{M_A^{(\alpha)}}\right) + \left(\frac{\Delta M_B^{(\alpha)}}{M_B^{(\alpha)}}\right)\right]\widetilde{\delta}_{0,0}^{Li} - \Delta \widetilde{Y}_{0,0}^{(\alpha)}, \qquad (10)$$

where the tildes '~' over the various symbols indicate that they represent the differences between these quantities in the excited and in the reference (ground) electronic state [see, e.g., Eq. (6)].

In order to determine estimates of the physically interesting quantities $\Delta \widetilde{T}_e^{(\alpha)}$, the molecular constants in Tables II–VI have been used to generate the values of $Y_{0,0}^{(\alpha)}$ shown in columns 5–7 of Table VII. We note that the differences between these quantities for different isotopomers, $\Delta \widetilde{Y}_{0,0}^{(\alpha)}$, are quite small relative to the magnitude of the $\Delta T_{v=-1/2}^{(\alpha)}$ terms. Utilizing these results in the above expressions yields the isotopomer-dependent relative electronic state energies shown in the last two columns of Table VII. No empirical BOB terms could be determined for the $(5p)\,{}^1\Pi_u$ state because data are currently available for only one of its isotopomers, namely, ${}^7Li_2$.

TABLE VI. Dunham ($Y_{l,m}$) and Λ-doubling ($q_{l,m}$) parameters for the Rydberg ${}^1\Pi_u$ state, derived from levels $v=0$ and 1 only, quoted in cm^{-1}. Λ doubling is calculated as $\pm(1/2)q_{0,1}J(J+1)$ with respect to a midpoint reference, and the e levels are higher than f levels for this state. Parameters for ${}^7Li_2$ are quoted with two standard deviation uncertainties (given in parenthesis) in units of the last digit shown.

Parameter	Fitted value ${}^7Li_2$	Calculated value ${}^6Li_2$	Calculated value ${}^6Li\,{}^7Li$
$\widetilde{T}_{v=-1/2}$	37 258.988(7)	[37 258.988][a]	[37 258.988][a]
$Y_{1,0}$	262.441(7)	283.435 58	273.140 08
$Y_{0,1}$	0.510 804(56)	0.595 798 85	0.553 301 43
$10^3\,Y_{1,1}$	−9.33(7)	−11.753	−10.5182
$10^6\,Y_{0,2}$	−7.78(8)	−10.5845	−9.1284
$10^9\,Y_{0,3}$	−0.97(5)	−1.5392	−1.2328
$10^5\,q_{0,1}$	2.4(7)	3.27	2.82

[a]Electronic isotope shifts cannot be determined since data are only available for the ${}^7Li_2$ isotopomer.

TABLE VII. Born-Oppenheimer breakdown parameters, semiclassical zero-point energy corrections $Y_{0,0}$ [from Eq. (7)], and electronic state energies and isotope shifts for the $X\,^1\Sigma_g^+$, $A\,^1\Sigma_u^+$, $B\,^1\Pi_u$, and $1\,^1\Delta_g$ states of Li$_2$, all in cm^{-1}. The uncertainties in $\tilde{T}_e$ (^{7}Li$_2$) are those for $\tilde{T}_{v=-1/2}$ given in Tables II–V, since contributions from the uncertainties in $Y_{0,0}$ are much smaller.

| | | | | $Y_{0,0}$ | | | $\tilde{T}_e$ | $\Delta\tilde{T}_e$ | |
State	$\tilde{\delta}_{0,0}$	$10^3\times\delta_{1,0}$	$10^5\times\delta_{0,1}$	[^{7}Li$_2$]	[^{6}Li$_2$]	[^{6}Li ^{7}Li]	[^{7}Li$_2$]	[^{6}Li$_2$]	[^{6}Li ^{7}Li]
$X\,^1\Sigma_g^+$	0.0	5.6(5)	a	−0.0311(2)	−0.0363(4)	−0.0337(3)	0.0	0.0	0.0
$A\,^1\Sigma_u^+$	0.346(4)	7.8(5)	7.5(2)	+0.0746(3)	+0.0870(4)	+0.0808(3)	14 068.194	−0.133	−0.066
$B\,^1\Pi_u$	0.685(4)	a	a	−0.0582(10)	−0.0679(15)	−0.0631(12)	20 436.272	−0.223	−0.112
$1\,^1\Delta_g$	1.339(5)	a	−7.4(4)	−0.1024(3)	−0.1194(4)	−0.1109(3)	28 746.381	−0.434	−0.217

[a]A physically significant value of this parameter could not be determined.

V. CONCLUSION

This paper reports a systematic determination of Born-Oppenheimer breakdown effects in a stack of several different electronic states of a single chemical species. This was made possible by a simultaneous combined-isotopomer treatment of a wealth of data, coupling five different electronic states. We find that the dominant Born-Oppenheimer breakdown effect in the neighborhood of the equilibrium internuclear distances in these excited electronic states of Li$_2$ is an additive energy shift which approximately doubles from the $A\,^1\Sigma_u^+$ to the $B\,^1\Pi_u$ state, and again from the $B\,^1\Pi_u$ to the $1\,^1\Delta_g$ state. The doubling from the $B\,^1\Pi_u$ to the $1\,^1\Delta_g$ state may be naively explained by the fact that the dominant configuration of Li$_2(B\,^1\Pi_u)$ is (Li $2s+$Li $2p$) and that of Li$_2(1\,^1\Delta_g)$ is (Li $2p+$Li $2p$), whilst the smaller value for the $A\,^1\Sigma_u^+$ state could be attributed to its being more strongly affected by configuration mixing.

The fact that the effective electronic isotope shifts for the A and B states seen in Table VII have distinctly smaller magnitudes than the known $2p\leftarrow 2s$ atomic isotope shift of -0.33 cm^{-1},[2] and the fact that the electronic isotope shift parameters in Table VII are differences from ground-state values, remind us that the present ''parameter-fit'' analysis does not yield a complete description of even the leading higher-order BOB parameters for this species. To obtain T_e and ΔT_e values without the ''tilde'' superscript will require the experimental determination of the absolute difference in the well depths for different isotopomers in at least one of these electronic states. Future work will address this limitation by utilizing $A\,^1\Sigma_u^+$ state data extending almost to dissociation, and by applying direct-potential-fit methods to determine analytical functions for $V(R)$, Λ-doubling, and BOB functions.

[1] X. Wang, J. Magnes, A. M. Lyyra, A. J. Ross, F. Martin, P. M. Dove, and R. J. Le Roy, J. Chem. Phys. **117**, 9339 (2002).
[2] C. J. Sansonetti, B. Richou, R. Engleman, Jr., and L. J. Radziemski, Phys. Rev. A **52**, 2682 (1995).
[3] Y. Huang and R. J. Le Roy, J. Chem. Phys. **119**, 7398 (2003).
[4] C. Linton, F. Martin, P. Crozet, A. J. Ross, and R. Bacis, J. Mol. Spectrosc. **158**, 445 (1993).
[5] R. J. Le Roy, J. Mol. Spectrosc. **194**, 189 (1999).
[6] N. Bouloufa, P. Cacciani, R. Vetter, A. Yiannopoulou, F. Martin, and A. J. Ross, J. Chem. Phys. **114**, 8445 (2001).
[7] N. Bouloufa, P. Cacciani, V. Kokouline, F. Masnou-Seeuws, R. Vetter, and L. Li, Phys. Rev. A **63**, 042507 (2001).
[8] M. M. Hessel and C. R. Vidal, J. Chem. Phys. **70**, 4439 (1979).
[9] A. J. Ross, P. Crozet, C. Linton, F. Martin, I. Russier, and A. Yiannopoulou, J. Mol. Spectrosc. **191**, 28 (1998).
[10] A. J. Ross, F. Martin, A. Adohi-Krou, and C. Jungen, J. Mol. Spectrosc. (to be published).
[11] See EPAPS Document No. E-JCPSA6-121-003436 for ascii files containing line measurements used in the present work. A direct link to this document may be found in the online article's HTML reference section. The document may also be reached via the EPAPS homepage (http://www.aip.org/pubservs/epaps.html) or from ftp.aip.org in the directory /epaps/. See the EPAPS homepage for more information.
[12] R. J. Le Roy, University of Waterloo Chemical Physics Research Report CP-658, 2004; http://leroy.uwaterloo.ca
[13] E. R. I. Abraham, N. W. M. Ritchie, W. I. Alexander, and R. G. Hulet, J. Chem. Phys. **103**, 7773 (1995).
[14] C. Linton, F. Martin, I. Russier, A. J. Ross, P. Crozet, S. Churassy, and R. Bacis, J. Mol. Spectrosc. **175**, 340 (1996).
[15] K. Urbanski, S. Antonova, A. Yiannopoulou, A. M. Lyyra, L. Li, and W. C. Stwalley, J. Chem. Phys. **104**, 2813 (1996); **116**, 10577(E) (2002).
[16] J. L. Dunham, Phys. Rev. **41**, 721 (1932).
[17] A. Pashov, W. Jastrzebski, and P. Kowalczyk, J. Chem. Phys. **113**, 6624 (2000).
[18] S. Antonova, G. Lazarov, K. Urbanski, A. M. Lyyra, L. Li, G.-H. Jeung, and W. C. Stwalley, J. Chem. Phys. **112**, 7080 (2000).
[19] R. Bernheim, L. P. Gold, and T. Tipton, J. Chem. Phys. **78**, 3635 (1983).
[20] X. Wang, J. Yang, J. Qi, and A. M. Lyyra, J. Mol. Spectrosc. **191**, 295 (1998).
[21] D. K. Hsu, Ph.D., Fordham University, 1975.